Abscisic acid regulates secondary cell-wall formation and lignin deposition in *Arabidopsis thaliana* through phosphorylation of NST1

Chang Liu[a,b,1], Hasi Yu[a,b,1], Xiaolan Rao[a], Laigeng Li[b], and Richard A. Dixon[a,2]

[a]BioDiscovery Institute and Department of Biological Sciences, University of North Texas, Denton, TX 76203; and [b]National Key Laboratory of Plant Molecular Genetics & CAS Center for Excellence in Molecular Plant Sciences, Shanghai Institute of Plant Physiology and Ecology, Chinese Academy of Sciences, Shanghai 200032, China

Contributed by Richard A. Dixon, September 13, 2020 (sent for review May 29, 2020; reviewed by Zhizhong Gong, Yuanyue Shen, and Jack P. Wang)

Plant secondary cell-wall (SCW) deposition and lignification are affected by both seasonal factors and abiotic stress, and these responses may involve the hormone abscisic acid (ABA). However, the mechanisms involved are not clear. Here we show that mutations that limit ABA synthesis or signaling reduce the extent of SCW thickness and lignification in *Arabidopsis thaliana* through the core ABA-signaling pathway involving SnRK2 kinases. SnRK2.2. 3 and 6 physically interact with the SCW regulator NAC SECONDARY WALL THICKENING PROMOTING FACTOR 1 (NST1), a NAC family transcription factor that orchestrates the transcriptional activation of a suite of downstream SCW biosynthesis genes, some of which are involved in the biosynthesis of cellulose and lignin. This interaction leads to phosphorylation of NST1 at Ser316, a residue that is highly conserved among NST1 proteins from dicots, but not monocots, and is required for transcriptional activation of downstream SCW-related gene promoters. Loss of function of NST1 in the *snd1* mutant background results in lack of SCWs in the interfascicular fiber region of the stem, and the Ser316Ala mutant of NST1 fails to complement this phenotype and ABA-induced lignin pathway gene expression. The discovery of NST1 as a key substrate for phosphorylation by SnRK2 suggests that the ABA-mediated core-signaling cascade provided land plants with a hormone-modulated, competitive desiccation-tolerance strategy allowing them to differentiate water-conducting and supporting tissues built of cells with thicker cell walls.

secondary cell wall | drought response | posttranslational modification | lignification | hormone signaling

Plant cells are enclosed in cell walls. Cells undergoing elongation possess thin primary walls that are composed mainly of cellulose, hemicellulose, and pectin (1). Some specific cell types deposit thicker secondary cell walls (SCWs) after cessation of elongation that empower these specialized cells with unique functions, such as mechanical support, long distance conduction of water and nutrients, resistance to biotic stress, pod shedding, and pollen release (2). SCWs are composed mainly of cellulose, lignin, and hemicellulose (3).The lignocellulose in the SCW represents the most abundant biomass on the planet for forage and potential biofuel production (4).

The formation of the thickened SCW is strictly controlled by a hierarchical transcriptional network (5). A group of closely related NAC domain transcription factors (TFs) function at the top of this network. These secondary-wall–associated NACs have been shown to regulate a battery of downstream TFs such as MYB TFs, which in turn regulate the biosynthetic genes for SCW deposition (6). Recent studies have found several genes which can influence SCW deposition through regulating other genes in this network (7). However, the upstream players that participate in the regulation of the first-layer TFs remain largely unknown.

During their entire lives, plants are exposed to various environmental stresses. The process of SCW deposition is responsive to stress and is controlled by a wide variety of factors both exogenous (photoperiod and temperature) and endogenous (phytohormones) and by interactions between them. In temperate latitudes, active and dormant states of the cambium of woody plants cause a distinct annual ring structure with a characteristic early wood/late-wood pattern. Wood formed at the beginning of the growing season is composed of cells with large diameters in the radial direction and thin cell walls. In the latter half of the growing season it is composed of cells with small diameters and thick cell walls (8). In *Pinus radiata* and *Pinus sylvestris*, late-wood formation is correlated with an increase in the concentration of the plant hormone abscisic acid (ABA) (9, 10). In *Arabidopsis*, ABA treatment results in the up-regulation of SCW-associated NACs (11). These results indicate that ABA is involved in SCW formation, but the molecular mechanisms underlying its exact role remain unclear.

ABA functions in plants through recognition by members of the intracellular PYL receptor family. The ABA-bound PYLs form complexes with the clade A PP2C phosphatases, allowing release of the inhibition of Snf1 (sucrose nonfermenting 1)-Related Kinase (SnRK2) protein kinases caused by dephosporylation by PP2Cs. SnRK2s, which act as a central hub in ABA signaling, are then activated through autophosphorylation (12). SnRK2s regulate multiple physiological responses through phosphorylating target substrates including ion channels (SLAC1, KAT1) (13, 14) and TFs (ABI5, ABFs) (15, 16). In the absence of ABA,

Significance

Lignin deposition in plants is affected by environmental stress, and stress-signaling involves increases in the levels of the plant hormone abscisic acid (ABA). Here we show, using a combination of biochemical and genetic approaches, how ABA can regulate lignin biosynthesis. This involves phosphorylation of the master lignin transcription factor NST1 by a family of protein kinases (SnRK2s) that are themselves activated by phosphorylation as a result of ABA recognition by its receptor. This work provides a basis for designing trees and other biomass plants that are better adapted to stress and climate change.

Author contributions: C.L., H.Y., L.L., and R.A.D. designed research; C.L. and H.Y. performed research; C.L., H.Y., X.R., and L.L. analyzed data; and C.L., H.Y., and R.A.D. wrote the paper.

Reviewers: Z.G., China Agricultural University; Y.S., Beijing University of Agriculture; and J.P.W., North Carolina State University.

The authors declare no competing interest.

[1]C.L. and H.Y. contributed equally to this work.

[2]To whom correspondence may be addressed. Email: richard.dixon@unt.edu.

This article contains supporting information online at https://www.pnas.org/lookup/suppl/doi:10.1073/pnas.2010911118/-/DCSupplemental.

Published January 25, 2021.

PP2Cs dephosphorylate and thereby inactivate SnRK2s to block ABA signaling (12).

Here, we demonstrate reduced lignified SCW formation in *Arabidopsis thaliana* in response to genetic blocks in ABA synthesis and sensing. The protein kinase SnRK2, a key positive regulator of ABA signaling, can interact with and phosphorylate AtNST1, a master TF which enhances SCW formation and lignin deposition in the stem fiber region. Accordingly, point mutations in the SnRK2-mediated phosphorylation site of AtNST1 abolish the TF regulatory activity. Thus, we have uncovered a mechanism for how ABA signaling modulates SCW thickening in *Arabidopsis*.

Results

Loss of Function of ABA2 or SnRK2.2/3/6 Interferes with SCW Deposition in *Arabidopsis*. *ABA2* encodes a short-chain dehydrogenase. Loss of function of *ABA2* blocks the conversion of xanthoxin to ABA-aldehyde which leads to a reduced level of endogenous ABA during various stages of plant and seed development (17). Three SNF1-related protein kinase 2s—SnRK2.2, SnRK2.3 and SnRK2.6—are positive effectors of the ABA response. In *Arabidopsis*, a triple mutant of the three ABA-regulated SnRK2s is strongly ABA-insensitive (15, 18).

Interrogation of the *Arabidopsis* eFP Browser (19), the online database of gene expression during *Arabidopsis* development, showed that the transcripts of ABA2, SnRK2.2, and SnRK2.6 were highly accumulated in the second internode of inflorescence stems which are rich in vascular tissues that undergo SCW thickening, whereas SnRK2.3 transcripts were less highly accumulated (*SI Appendix*, Fig. S1). This is in accordance with previous observations that showed high expression levels of ABA2 and SnRK2s in stems or vascular tissues of *Arabidopsis* (16, 20, 21).

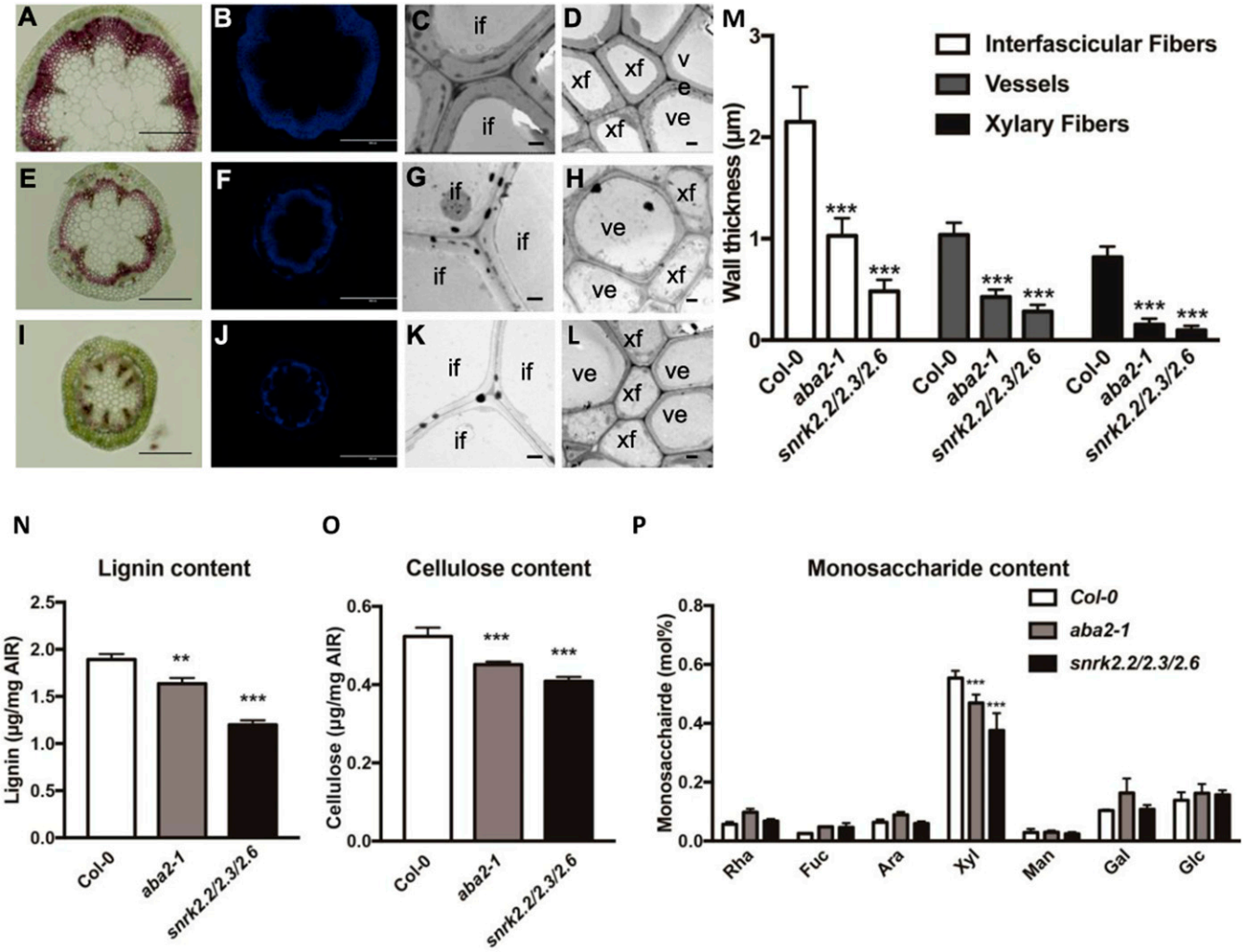

Fig. 1. Inhibition of SCW thickening in ABA synthesis and signaling mutants. (*A*–*L*) Cross-sections of the stems of wild-type (WT, Col-0), *aba2-1*, and *snrk2.2/snrk2.3/snrk2.6* mutant plants. (*A*, *E*, and *I*) Cross-sections of the stems of WT (*A*), *aba2-1* mutant (*E*), and *snrk2.2/snrk2.3/snrk2* mutant (*I*) with phloroglucinol staining. (*B*, *F*, and *J*) Cross-sections of the stems of WT (*B*), *aba2-1* mutant (*F*), and *snrk2.2/snrk2.3/snrk2* mutant (*J*) under UV autofluorescence. (*C*, *G*, and *K*) Transmission electron micrographs of interfascicular fiber cells of WT (*C*), *aba2-1* mutant (*G*), and *snrk2.2/snrk2.3/snrk2.6* mutant (*K*) plants. (*D*, *H*, and *L*) Transmission electron micrographs of xylem cells of WT (*D*), *aba2-1* mutant (*H*), and *snrk2.2/snrk2.3/snrk2* mutant (*L*) plants. (*M*) Wall thickness of vessels and fibers in the inflorescence stems of WT, *aba2-1*, and *snrk2.2/snrk2.3/snrk2.6*. (*N* and *O*) Contents of lignin (*N*) and crystalline cellulose (*O*) in the inflorescence stems of WT, *aba2-1*, and *snrk2.2/snrk2.3/snrk2.6*. (*P*) Monosaccharide content of alcohol-insoluble cell-wall residues from in the inflorescence stems of WT, *aba2-1*, and *snrk2.2/snrk2.3/snrk2.6*. Data in *M* represent average values ± SD ($n = 24$ cells from three independent plants). In *N*–*P*, relative levels of the indicated transcripts are normalized to ACT2. The transcript level of genes of interest in WT plants was set to 1. Data represent average values ± SD ($n = 4$ biological replicates). Asterisks indicate significant differences from Col-0 (**$P < 0.05$; ***$P < 0.0001$) by pairwise comparison Tukey's test. if: interfascicular fiber; ve: vessel; xf: xylary fiber. (Scale bars: 400 μm in *A*, *B*, *E*, *F*, *I*, and *J*; 2 μm in *C*, *D*, *G*, *H*, *K* and *L*.)

Therefore, to determine whether changes in ABA content and ABA signal transduction affect SCW deposition and lignification in *A. thaliana*, we first examined the inflorescence stems of *aba2-1* mutant and *snrk2.2/3/6* triple-mutant plants by microscopy to localize phloroglucinol staining and ultraviolet (UV) autofluorescence, both of which detect lignin. The *aba2-1* allele has a single amino acid substitution, resulting in ~10% residual enzymatic activity (17). Slightly altered SCW deposition and lignification were seen in both the xylem vessels and fibers in the *aba2-1* mutant, whereas severe defects in SCW deposition and lignification were observed in *snrk2.2/3/6* triple-mutant plants (Fig. 1 *A*, *B*, *E*, *F*, *I*, and *J*). Transmission electron microscopy confirmed that both *aba2-1* mutant and *snrk2.2/3/6* triple-mutant plants displayed thinner cell walls in fiber and vessel cells compared to wild-type plants (Fig. 1 *C*, *D*, *G*, *H*, *K*, and *L*). The decrease in SCW thickness was greater in the *snrk2.2/3/6* triple mutant than in the *aba2-1* mutant (Fig. 1*M*).

To investigate changes in SCW components in the *aba2-1* and *snrk2.2/3/6* mutants, we analyzed total lignin and crystalline cellulose contents, as well as monosaccharide composition of the cell wall matrix, in inflorescence stems (Fig. 1 *N*–*P*). Significant reductions in the contents of lignin and crystalline cellulose between *aba2-1* and *snrk2.2/3/6* mutants and wild-type plants were observed (Fig. 1 *N* and *O*). The amounts of total lignin and cellulose were lower in *snrk2.2/3/6* than in *aba2-1* plants (Fig. 1 *N* and *O*). Reduction in the content of xylose from noncellulosic polysaccharides was found in both the *aba2-1* mutant and *snrk2.2/3/6* triple mutant compared to wild-type plants (Fig. 1*P*). Thus, disruption of both ABA biosynthesis or ABA signaling result in alterations in SCW deposition and composition.

Loss of Function of ABA2 or SnRK2.2/3/6 Affects Transcript Levels of SCW-Related Genes. To address how alteration of ABA content or signaling interferes with SCW deposition, we first examined the transcript levels of SCW-related genes in the *aba2-1* and *snrk2.2/3/6* triple-mutant plants. The 13 selected SCW-related genes included four master transcription factors (*SND1*, *NST1*, *MYB46*, and *MTB83*), three xylan biosynthesis genes (*IRX8*, *IRX9*, and *IRX14*), three lignin biosynthesis genes (*PAL1*, *CCoAOMT*, and *4CL1*), and three SCW cellulose synthase genes (*CesA4*, *CesA7*, and *CesA8*) (7, 22, 23). Transcript levels of all selected genes were reduced in the stems of *aba2-1* mutant plants (Fig. 2). Surprisingly, although the decrease in SCW thickness is greater in stems of the *snrk2.2/3/6* triple mutant than in the *aba2-1* mutant, the SCW-related gene transcript levels in stems of the *snrk2.2/3/6* triple mutant were reduced less than in the *aba2-1* mutant. In fact, the transcript levels of SND1, CESA4, and CESA7 were higher than in wild-type plants (Fig. 2). Together, these data indicate that ABA deficiency has greater effects on transcripts associated with SCW deposition than does lack of sensitivity to ABA.

NCED encodes a 9-*cis*-epoxycarotenoid dioxygenase, which cleaves 9-*cis*-epoxycarotenoids to produce xanthoxin (24). NCED expression is a major determinant of ABA accumulation, and overexpression of NCED leads to increased ABA levels (25, 26). To further address the regulation of SCW deposition by ABA, we examined the inflorescence stems and SCW-related gene expression in two NCED overexpressing lines of *A. thaliana*, NCED6-OX and NCED9-OX (*SI Appendix*, Fig. S2*A*). Microscopic examination of phloroglucinol staining and UV autofluorescence showed no significant alteration in the SCWs of vessel and fiber cells in NCED6-OX and NCED9-OX lines (*SI Appendix*, Fig. S2 *B* and *C*). However, the 13 selected genes representing SCW transcription factors and enzymes involved in hemicellulose, lignin, and cellulose biosynthesis were all upregulated in the stems of NCED6-OX and NCED9-OX lines (*SI Appendix*, Fig. S2*D*). Together with the inconsistency between SCW gene transcript levels and phenotypic response in the *snrk2.2/3/6* triple mutant, these results suggest the involvement of posttranscriptional mechanisms in ABA-mediated regulation of SCW deposition.

SnRK2.2/3/6 Interact With NAC SECONDARY WALL THICKENING PROMOTING FACTOR 1. The integral ABA-signaling module relies on SnRK2 activation and SnRK2's subsequent phosphorylation of target proteins (12). Loss of function of SnRK2.2/3/6 results in reduced phosphorylation of SnRK target proteins (27). The potential involvement of posttranscriptional regulation in SCW thickening via ABA signaling suggests a role for SnRK2 phosphorylation in this process. To determine if there is a substrate for phosphorylation by SnRK2 that is involved in SCW formation, we performed yeast two-hybrid screens. A complementary DNA (cDNA) library of *A. thaliana* inflorescence stems undergoing SCW formation was screened against SnRK2.6 protein. Among the positive clones, NAC SECONDARY WALL THICKENING PROMOTING FACTOR 1 (NST1) (Fig. 3*A*) was of particular interest as this is a member of a previously described family of NAC transcription factors controlling the expression of SCW biosynthetic genes (28, 29). We also retrieved a phosphopeptide ([pS] PYPSLNR) of the NST1 protein from the PhosPhAt database which provides mass-spectrometry–based identification of phosphorylation sites in *Arabidopsis* proteins (30) (*SI Appendix*, Fig. S3). Together, these results suggest that NST1 might be a target of SnRK2 in *Arabidopsis*.

To confirm whether NST1 interacts with all three SnRK2 proteins, a construct for expression of NST1 in PGBK-T7 vector was cotransformed into yeast with constructs for expression of SnRK2.2, SnRK2.3, or SnRK2.6 fused to PGAD-T7 vector, respectively, and the transformants were tested for their ability to grow on selective plates. Only those yeast cells containing NST1 in combination with SnrK2.2, SnrK2.3, or SnrK2.6 were able to grow on media depleted of leucine, threonine, and histidine (-L-T-H), indicating that NST1 interacts with SnRK2.2, SnRK2.3, and SnRK2.6 (Fig. 3*A*). To further confirm the interaction of NST1 with the three SnRK2s, an in vitro binding assay was performed. Glutathione-Sepharose beads with immobilized glutathione-*S*-transferase (GST) or NST1-GST fusion protein were incubated with purified SnRK2s-His fusion proteins. The bound protein complexes were then eluted from the beads by incubation with reduced glutathione and separated on a sodium dodecyl sulfate (SDS) gel. The results showed that all three SnRK2s bound to NST1-GST but not to GST alone (Fig. 3*B*). To confirm interaction of NST1 with the three SnRK2s in vivo, a bimolecular fluorescence complementation assay was performed. NST1 and SnRK2s were fused to unfolded complementary fragments of yellow fluorescent protein (YFP) reporter, and the resulting plasmids and empty vectors were introduced into tobacco leaves by agro-infiltration as described previously (31). The fluorescent signal of the protein complexes was detected by confocal fluorescence microscopy. YFP signal was observed only in the nuclei of cells expressing both NST1 and SnRK2 fusion proteins (Fig. 3*C*). Taken together, these results indicate that NST1 interacts with SnRK2.2, SnRK2.3, and SnRK2.6 in the nucleus.

SnRK2.2/3/6 Phosphorylate NST1 at Ser-316 In Vitro. According to the PhosPhAt database, NST1 contains a phosphopeptide with S316 as the phosphorylated residue (*SI Appendix*, Fig. S3). To determine whether SnRK2.2, SnRK2.3, and SnRK2.6 can phosphorylate NST1 on S316, we expressed the three SnRK2-His fusion proteins in *Escherichia coli*, purified the kinases, and incubated them individually with recombinant fusion proteins of NST1-GST or NST1 (S316A)-GST, a variant NST1 generated by a mutation lacking the phosphorylation site on residue 316. Antibodies to phosphoserine were used to immuno-detect phosphorylated proteins (Fig. 4). The results showed that

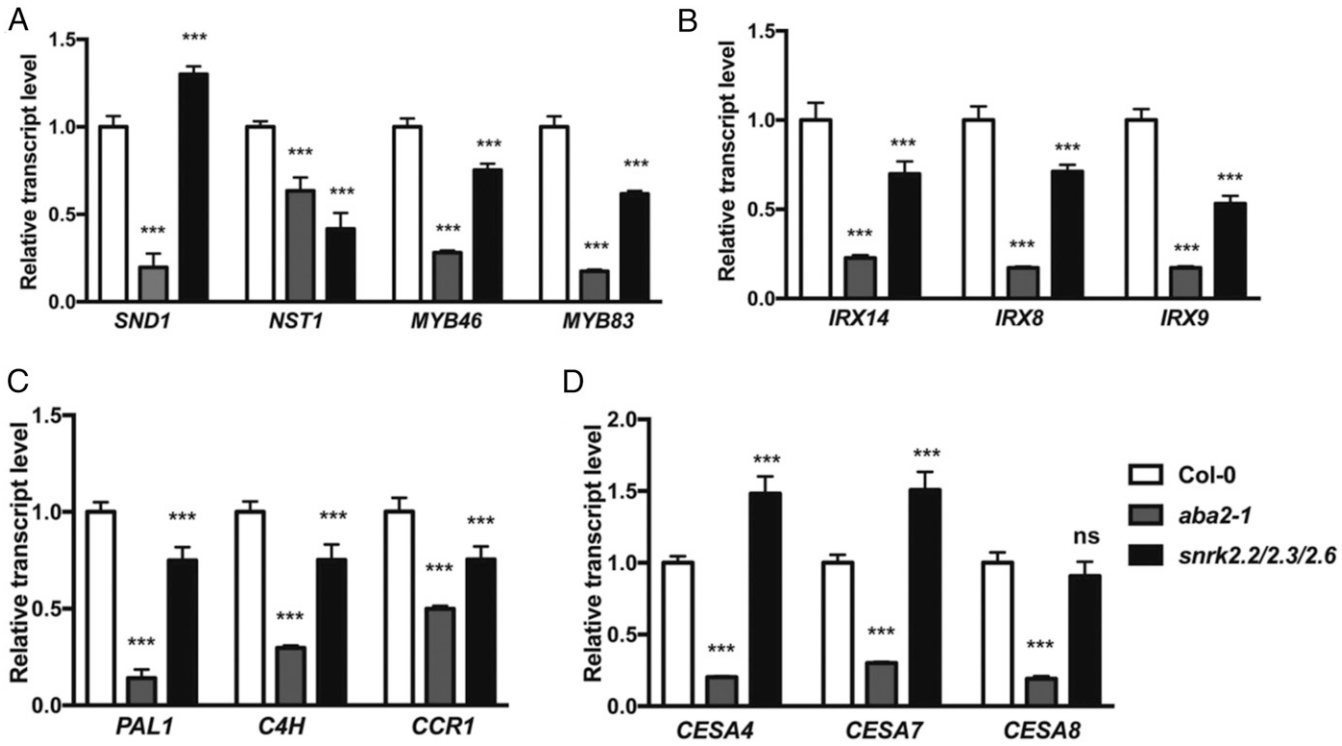

Fig. 2. Suppressed expression of genes related to SCW synthesis in ABA mutants. (*A–D*) Transcript levels of SCW synthesis-associated genes in the basal first and second internodes of inflorescence stems of Col-0, *aba2-1*, and *snrk2.2/snrk2.3/snrk2.6* plants. Relative levels of the indicated transcripts are normalized to ACT2. The WT transcript level of genes of interest was set to 1. Data represent average values ± SD ($n = 4$ biological replicates in *A–D*). Asterisks indicate significant differences from Col-0 (***$P < 0.0001$) by pairwise comparison Tukey's test. ns, not significant.

purified SnRK2s isolated from *E. coli* were active and autophosphorylated (Fig. 4 *A–C*, lane 1). This could be the result of the lack of PP2C proteins in *E. coli* because, in plants, these proteins dephosphorylate SnRK2s and render them inactive. NST1 was phosphorylated in vitro by all three SnRK2 proteins (Fig. 4 *A–C*, lane 5); however, this was largely blocked by substitution of S316 by A (Fig. 4 *A–C*, lane 6), although a small level of phosphoserine was detected in the S316A mutant protein after incubation with SnRK2.2 and SnRK2.6, suggesting the possibility of an additional "weak" phosphorylation site. As also seen in Fig. 3*B*, the NST1-GST fusion protein generated a number of degradation products on SDS/polyacrylamide gel electrophoresis (PAGE).

SnRK2.2/3/6-Mediated Phosphorylation of NST1 Affects Its Transcriptional Activity in SCW Thickening in an ABA-Dependent Manner. To determine whether the phosphorylation of NST1 affects SCW thickening in *Arabidopsis*, we generated transgenic plants expressing NST1 or NST1(S316A) under control of the native NST1 promoter in the *nst1/snd1* double mutant background. Both proteins were similarly accumulated in these plants, indicating that phosporylation of NST1 at S316 does not significantly affect the stability of the protein (*SI Appendix*, Fig. S4). Plants of independent T2 homozygous lines were used for phenotypic evaluation (Fig. 5). NST1 and SND1 function redundantly in regulation of SCW synthesis, and T-DNA knockout mutation of both SND1 and NST1 specifically blocks SCW thickening in interfascicular and xylary fibers in *Arabidopsis* stems but has no effect on vessels. Loss of function of SND1 and NST1 results in a pendent stem phenotype compared with the upright growth of wild-type stems and *snd1* single T-DNA knockout mutant stems (28, 32) (Fig. 5*A*). The defective phenotype of pendent stems was reversed to normal phenotype in the pNST1:NST1 *nst1/snd1* transgenic lines. In contrast, the pNST1:NST1(S316A) *nst1/snd1* lines still exhibited a pendent stem phenotype (Fig. 5*A*). Phloroglucinol staining, UV autofluorescence observations, and measurements of wall thickness showed that the wild-type and *snd1* single-mutant stems developed thick-walled interfascicular fibers, xylary fibers, and vessels, whereas the *nst1/snd1* double-mutant stem had only thick-walled vessels but lacked secondarily thickened walls in both interfascicular and xylary fibers (Fig. 5 *B* and *C*). Expression of the pNST1:NST1 construct restored normal thick-walled fiber cells in the *nst1/snd1* double-mutant background. However, the above defects in SCW formation were not completely restored in the pNST1:NST1(S316A) *nst1/snd1* lines (Fig. 5 *B–D*). These results indicate that phosphorylation of NST1 positively regulates SCW thickening of fiber cells in *Arabidopsis*.

NST1 activates the expression of *MYB46* and *MYB83* through binding to their promoters (33, 34). We therefore examined whether phosphorylation of NST1 impacts its transactivation ability. We first confirmed the transactivation of the MYB46 and MYB83 promoters by NST1 in the dual luciferase system (Fig. 6 *A* and *B*) and showed that the S316A mutation reduced the activation of MYB46 and MYB83 by ~75 and 60%, respectively. The transcript level of NST1 in the *snrk2.2/3/6* triple mutant is lower than in the *aba2-1* mutant, in contrast to the other selected SCW genes which showed higher expression in *snrk2.2/3/6* than in *aba2-1* (Fig. 2). This suggests that loss of function of SnRK2 may result in reduced positive autoregulation of NST1, leading to its decreased expression. Dual luciferase assays showed the *trans*-activation of the NST1 promoter by NST1 itself (Fig. 6*C*), consistent with previous observations in yeast and plant cells (35, 36), and the S316A mutation reduced this activation by nearly 50%.

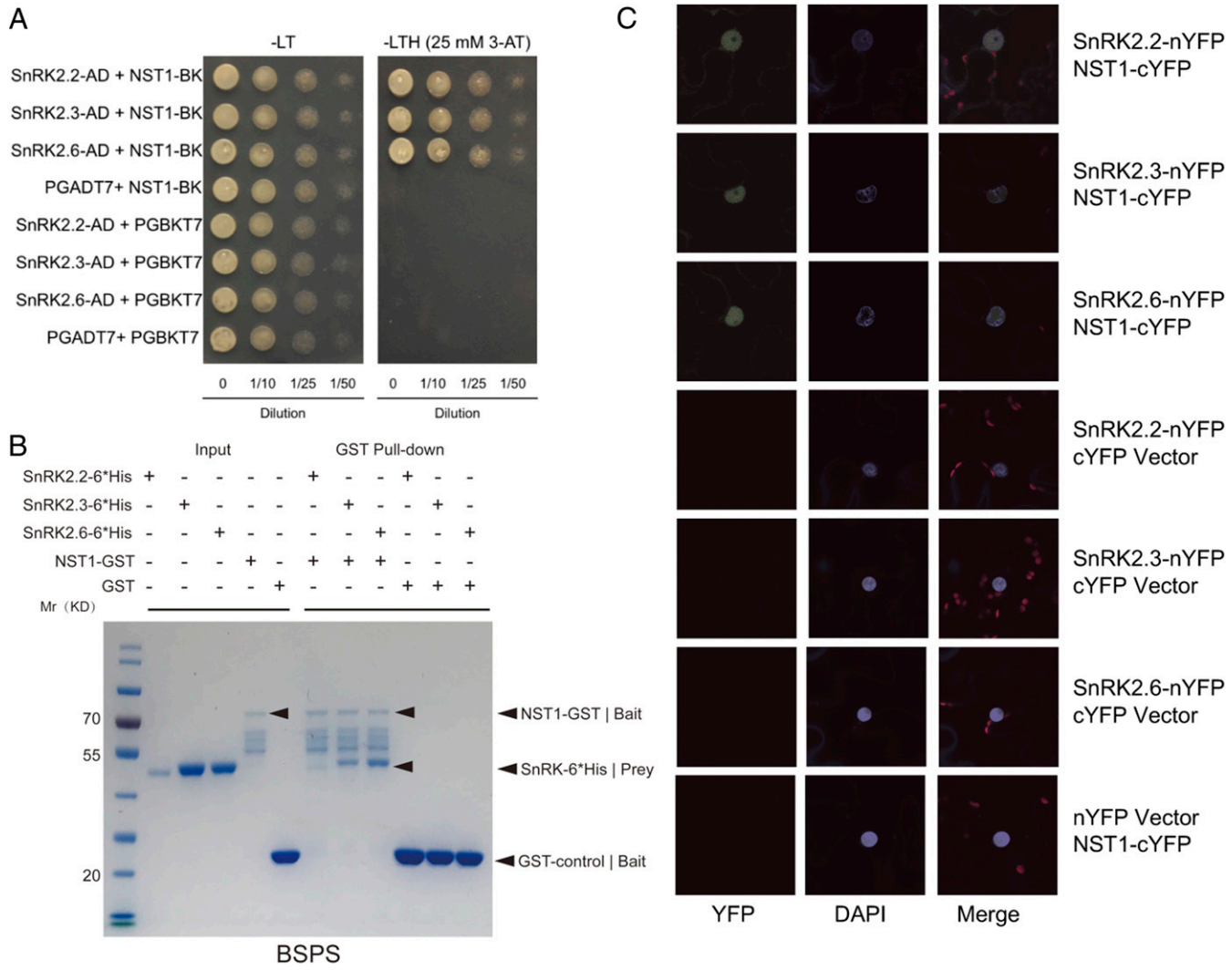

Fig. 3. NST1 interacts with SnRK2.2, SnRK2.3, and SnRK2.6 both in vitro and in vivo. (*A*) Yeast two-hybrid interaction assays reveal that NST1 interacts with *Arabidopsis* SnRK2.2, SnRK2.3, and SnRK2.6 when cells are cultured on SD/-Leu/-Thr/-His with 25 mM 3-AT (3-Amino-1,2,4-triazole). (*B*) In vitro pull-down assays showing the interaction of NST1-GST fusion protein and SnRK2s-6xHis fusion protein. NST1-GST and GST alone (control) were bound to Glutathione-Sepharose beads and incubated with SnRK2 proteins. After washing, complexes were removed from the beads by treatment with reduced glutathione, and proteins were separated by SDS/PAGE for 2 h under a constant voltage of 15 V per centimeter of gel length. The proteins were visualized by staining with Blue Safe Protein Stain (BSPS). (*C*) BiFC assay in tobacco leaves showing the interactions (revealed as fluorescence in the nucleus) between SnRK2.2, SnRK2.3, SnRK2.6, and NST1.

To further examine whether SnRK2-mediated phosphorylation of NST1 influences its downstream transcriptional function, we examined the *trans*-activation of the MYB46, MYB83, and NST1 promoters by NST1 using the dual luciferase system in protoplasts of both wild-type and *snrk2.2/3/6* triple-mutant plants (Fig. 6 *D*–*F*). NST1 showed significantly higher activation of the MYB46, MYB83, and NST1 promoters in protoplasts from wild-type *Arabidopsis* than from the *snrk2.2/3/6* triple mutant. Taken together, these results indicate that SnRK2.2/3/6-mediated phosphorylation of NST1 is a component of the transcriptional machinery regulating SCW thickening of fiber cells in *Arabidopsis*.

The activation of SnRK2.2/3/6 can also be triggered by osmotic stress in an ABA-independent manner (37–39) To determine whether ABA signaling is required for the SnRK2.2/3/6-mediated regulation of NST1 transcriptional ability, we first examined the expression of *MYB46* and *PAL4*, an NST1-regulated downstream lignin biosynthesis gene, in 10-d-old seedlings of wild-type *Arabidopsis* and *snrk2.2/3/6* triple mutant treated with ABA. Transcript levels of both *MYB46* and *PAL4* were induced in the wild-type plant, but failed to increase in the *snrk2.2/3/6* triple mutant upon ABA treatment (Fig. 6 *G* and *H*). The ABA-induced accumulation of *MYB46* and *PAL4* transcripts was partially impaired in the *nst1/snd1* double mutant (Fig. 6 *G* and *H*). However, the induction of both *MYB46* and *PAL4* by ABA treatment was restored to the wild-type level in the pNST1:NST1 *nst1/snd1* transgenic lines, but not in the pNST1:NST1(S316A) *nst1/snd1* lines (Fig. 6 *G* and *H*). The transcript level of the ABA-responsive gene *RD29A* was used as the positive control (Fig. 6*I*). These results suggest that the activation of NST1 triggered by the SnRK2.2/3/6-mediated phosphorylation is linked to ABA signaling.

To interrogate other SCW-related genes that can be up-regulated by ABA through the function of SnRK2.2/3/6, we carried out a meta-analysis of the publicly available microarray datasets for the *snrk2.2/3/6* triple mutant in the Genevestigator database (https://genevestigator.com/) (15). We found that 24 SCW-related genes were down-regulated in the *snrk2.2/3/6* triple mutant compared to the wild-type plant (*SI Appendix*, Fig. S5). Furthermore, in the wild-type plant, the transcript levels of these SCW-related

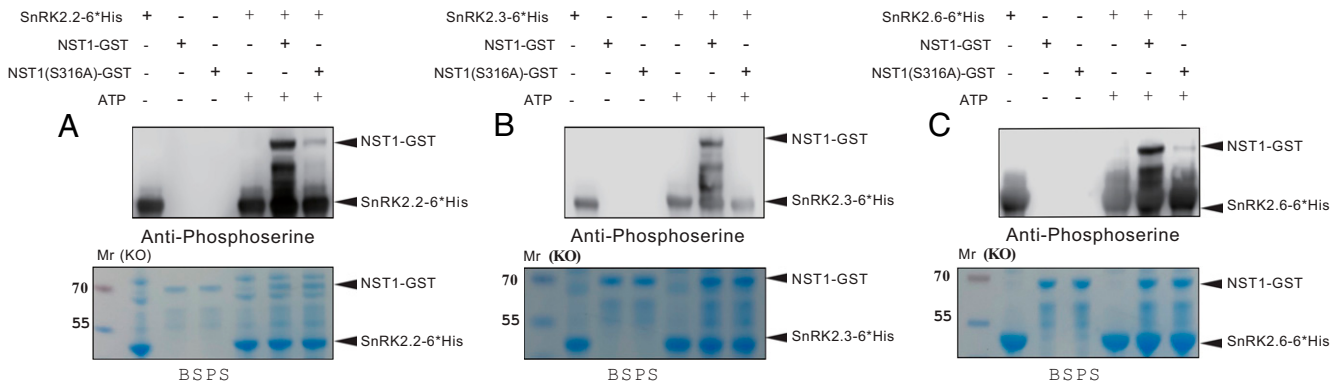

Fig. 4. SnRK2.2, SnRK2.3, and SnRK2.6 phosphorylate NST1 in vitro. Recombinant SnRK2 kinases (SnRK2s-6*His), NST1 (NST1-GST), and NST1$^{(S316A)}$ (NST1$^{(S316A)}$-GST) (a mutation with loss of the phosphorylation site) were isolated after expression in *E. coli* and used for phosphorylation assays. SnRK2.2 (*A*), SnRK2.3 (*B*), and SnRK2.6 (*C*) were incubated with wild-type or mutant NST1 and ATP at 30 °C for 2 h. The proteins were separated on an SDS/PAGE gel for 1 h under a constant voltage of 15 V per centimeter of gel length, and Western blotting was performed with antiphosphoserine antibody (*Upper*). The gels were stained with BSPS (*Lower*) for loading controls. Left lanes show M_r markers.

genes were induced after 90 min of ABA treatment, but to a lower level in the *snrk2.2/3/6* triple mutant (*SI Appendix*, Fig. S5). These results further indicate the involvement of ABA and SnRK2.2/3/6 in regulating SCW-related gene expression.

The Phosphorylation Site of NST1 Is Conserved in Dicotyledonous Plants. To determine whether the phosphorylation site of NST1 has been conserved during plant evolution, we first made blast alignments of NST1 amino acid sequences from 10 plant species in which NST1 orthologs have been functionally characterized. The motif LPSVRS(p) was conserved in the five dicot sequences (*SI Appendix*, Fig. S6*A*) but not in the five monocot sequences (*SI Appendix*, Fig. S6*B*), and the phosphorylated S residue was likewise present only in the homologous sequences of NST1 from dicots. By incorporating additional dicot protein sequences for motif analysis, we found that the S residue in the phosphorylation site of NST1 is conserved in several dicot plant protein sequences, and this residue is in the consensus sequence LRSSSS(p) (*SI Appendix*, Fig. S6*C*).

We then performed a phylogenetic analysis of 31 NST1 proteins from 13 different species. The phylogenetic tree (*SI Appendix*, Fig. S6*D*) showed three major clades differentiated by specific conserved domains. Proteins in the first clade (marked with a red star) showed high similarity to AtNST1, and all were from dicots. The proteins in the other two clades were less similar to AtNST1, and all were from monocots (*SI Appendix*, Fig. S6*D*). Thus, monocot NST1s are phylogenetically distinct from dicot NST1s and lack the phosphorylation site conferring ABA-signaling responsiveness.

Discussion

ABA Regulates SCW Deposition and Lignification in *Arabidopsis*. Both SCW deposition and lignification are reduced in the *aba2-1* and *snrk2.2/3/6* triple mutant; this, together with the loss of ABA-induction of SCW gene transcripts in the *snrk2.2/3/6* triple mutant, suggests that both endogenous ABA levels and the core ABA-signaling pathway are involved in normal SCW formation. ABA is the major hormone that controls a plant's ability to survive water-deficit stress, and the content of lignin is increased and lignin biosynthesis-related genes are up-regulated in several plant species under drought conditions (40–44). Additional lignification of conducting vessels under drought stress could allow the plant to maintain leaf or root turgor under a low-water potential due to the hydrophobic nature of lignins, thus preventing water loss to the apoplast (44–46). In addition, dehydration causes osmotic stress to plants, which can also activate SnRK2s through the activation of Raf-like kinases (47, 48). Future studies are needed to determine the detailed mechanisms that plant use to manage lignification and normal SCW formation under water-deficit conditions.

Overexpression of NCEDs in *A. thaliana* and *Populus deltoides* results in increased ABA content (26), and we show here that this induces expression of SCW-related genes. However, the extent and pattern of lignification and SCW deposition in stems of NCED overexpressing lines in the present work showed no significant changes compared to wild-type plants. It is therefore possible that additional mechanisms, involving interactions between ABA and other phytohormones and/or negative feedback regulation, protect these transgenic plants from overlignification. In contrast, in *P. deltoides* roots, NCED overexpression as a result of expressing the transcription factor NF-YB21 results in increased root growth associated with increased lignification and size of xylem vessels (49).

ABA Regulates SCW Deposition and Lignification in *Arabidopsis* at Both the Transcriptional and Posttranslational Levels. The observation that transcript levels of SCW-related genes are down-regulated in the *aba2-1* mutant but up-regulated in NCED overexpressing lines is consistent with previous results showing that exogenously applied ABA can up-regulate SCW-related NAC TFs (11) and indicates that ABA content can regulate SCW formation at the transcriptional level. At the same time, the *snrk2.2/3/6* triple mutant shows a more severe SCW-defective phenotype than the *aba2-1* mutant, although the transcript levels of SCW-related genes in the *snrk2.2/3/6* triple mutant are not uniformly down-regulated. This suggests posttranscriptional regulation of SCW formation by the core ABA-signaling pathway.

During the past 20 y, we have gained a clear understanding of the role of TFs in the regulatory network underlying SCW formation (7), but how the TFs themselves are regulated is less clear. Based on the present data, we propose a model (Fig. 7) that involves SnRK2-mediated phosphorylation of NST1, a master regulator of the transcription of downstream SCW-related genes. SnRK2 proteins are dephosphorylated and thereby inactivated by PP2C phosphatases. PP2C phosphatases are sequestered in the presence of ABA, thereby allowing autophosphorylation to convert the SnRK2 proteins to an active form that physically interacts with NST1 to catalyze its phosphorylation, restoring its function as a transcriptional activator of downstream SCW genes.

In addition to the posttranslational regulation of NST1, it has been known for some time that other TFs and downstream SCW

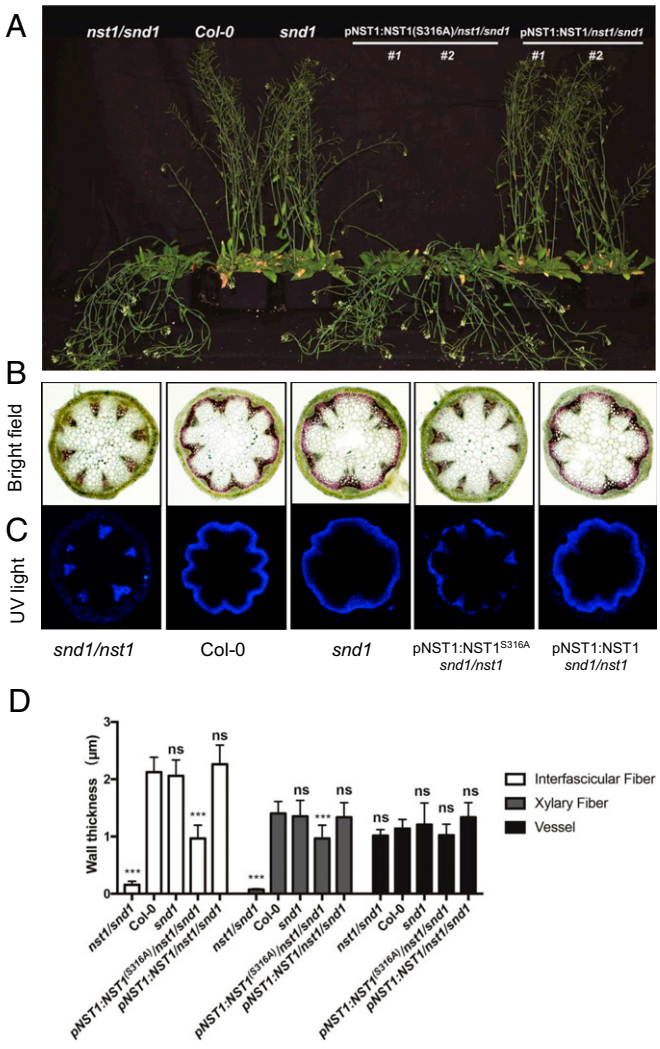

Fig. 5. The phosphorylation site of NST1 is essential for stem-cell-wall development and lignin deposition. (*A*) The 10-wk-old seedlings of *nst1/snd1*, Col-0 (wild type), *snd1*, pNST1:NST1$^{(S316A)}$/*nst1/snd1*, and pNST1:NST1/*nst1/snd1*. (*B*) Cross-sections of the stems of *nst1/snd1*, Col-0, *snd1*, pNST1:NST1$^{(S316A)}$/*nst1/snd1*, and pNST1:NST1/*nst1/snd1* under bright field. (*C*) Cross-sections of the stems of *nst1/snd1*, Col-0, *snd1*, pNST1:NST1$^{(S316A)}$/*nst1/snd1*, and pNST1:NST1/*nst1/snd1* under UV autofluorescence. (*D*) Cell-wall thickness of interfascicular fibers, xylary fibers, and vessels in the above lines. Data represent average values ± SD (n = 24 cells from three independent plants). Asterisks indicate significant differences from Col-0 (***P < 0.0001) by pairwise comparison Tukey's test. ns, not significant.

genes also undergo regulation via phosphorylation. This includes the phosphorylation of the TF E2Fc (50) and cellulose synthases (CESAs)1 and 7 in *Arabidopsis* (5, 51, 52), the phosphorylation of the MYB TF LTF1 in *Populus* (53), and the SUMOylation of the TF LBD30 in *Arabidopsis* (54). In a recent study, a quantitative atlas of the phosphoproteome of *Arabidopsis* was presented, and over 43,000 phosphorylation sites were found on 18,000 proteins (55). Among them, several lignin biosynthesis enzymes, including cinnamoyl CoA reductase, caffeic acid/5-hydroxyconiferaldehyde 3-*O*-methyltransferase (COMT), L-phenylalanine ammonia-lyase (PAL), and cinnamate 4-hydroxylase (C4H), have potential phosphorylation sites, and phosphorylation of PAL and COMT has been proposed to regulate the turnover or activities of these enzymes (56, 57). Whether these phosphorylations are catalyzed by SnRK2s or other related kinases in vivo remains to be determined. Such posttranslational modifications, however, may provide an explanation for the inconsistency between SCW-related transcript levels and SCW thickening in the different ABA synthesis and signaling mutants. It is also possible that ABA can regulate lignification in part by additional mechanisms not described here.

The Phosphorylation Site of NST1 Is Conserved in Dicots. NST1 belongs to the NAC TFs, one of the largest gene families in plants (58). These proteins are key regulators of stress perception and development, and most share a conserved N-terminal NAC domain but a highly divergent C-terminal transcriptional regulatory region which accounts for their diverse functions (59). For example, ANAC019 is a positive regulator of ABA signaling, and chimeric proteins, where the NAC domain of ANAC019 is replaced with the analogous regions from other NAC TFs, also have the ability to positively regulate ABA signaling (11). In contrast, replacing the ANAC019 C-terminal transcriptional regulatory region with the C-terminal regions from other NAC TFs abolished ANAC019-mediated ABA hypersensitivity (11). The phosphorylation site S316 of NST1 is present in the C-terminal region of the protein and is highly conserved among the dicots, but is not present in monocot NST1s, which are phylogenetically distinct from their dicot counterparts. It is also absent from SND1 (NST3), a gene that is functionally redundant with NST1 in regulating lignification of interfascicular fibers, but not the anther cell wall, in *A. thaliana* (29, 30, 33). Together, these data suggest a conserved role for the phosphorylation of NST1 in regulation of SCW formation in dicots, along with parallel pathways that may bypass the ABA-signaling–dependent route.

In a previous study of grass-secondary-wall–associated NACs, rice OsSWN1 and ZmSWN1, which are homologs of *Arabidopsis* NSTs in rice and maize, were able to rescue the pendent-stem phenotype conferred by the *Arabidopsis snd1/nst1* double mutant but failed to completely restore the stem strength (60). In another study, exogenous ABA arrested the growth of young rice shoots and inhibited SCW formation in sclerenchyma including expression of the cellulose synthase gene *OsCesA9* (61). Together, these results indicate different mechanisms for the regulation of SCW formation by ABA and NAC TFs in monocots and dicots, despite shared transcriptional targets of NST1. This situation may reflect the different organization, composition, and complexities of secondarily thickened tissues in the two groups of flowering plants.

The Development of Cell-Wall Thickening Is Associated with the Emergence of ABA-Dependent Responses in Land Plants. The emergence of water-conducting and supporting cells with thick cell walls is seen in the moss *Physcomitrella patens*, where it is regulated by NAC TFs that are similar to the SCW-associated NAC TFs of *A. thaliana* (62). An ABA-activated PYL receptor controlling a PP2C-SnRK2–dependent desiccation-tolerance pathway has also evolved in *P. patens* (63). Early diverging aeroterrestrial algae mount a dehydration response that is similar to that of land plants, but this does not depend on ABA (63). The evolution of ABA-mediated fine-tuning of the PP2C-SnRK2–signaling cascade provided land plants with a hormone-modulated, competitive desiccation-tolerance strategy allowing them to differentiate water-conducting and supporting tissues built of cells with thicker cell walls through endogenous ABA positively promoting SCW deposition in vessel and fiber cells. The ability for long-distance transport and mechanical support in turn conferred some desiccation tolerance during the adaption of plants to land (64). Why the underlying mechanism appears to be different in monocots and dicots remains unclear.

Materials and Methods

Detailed descriptions of additional experimental methods are provided in *SI Appendix, Supplementary Materials and Methods*. These include growth of

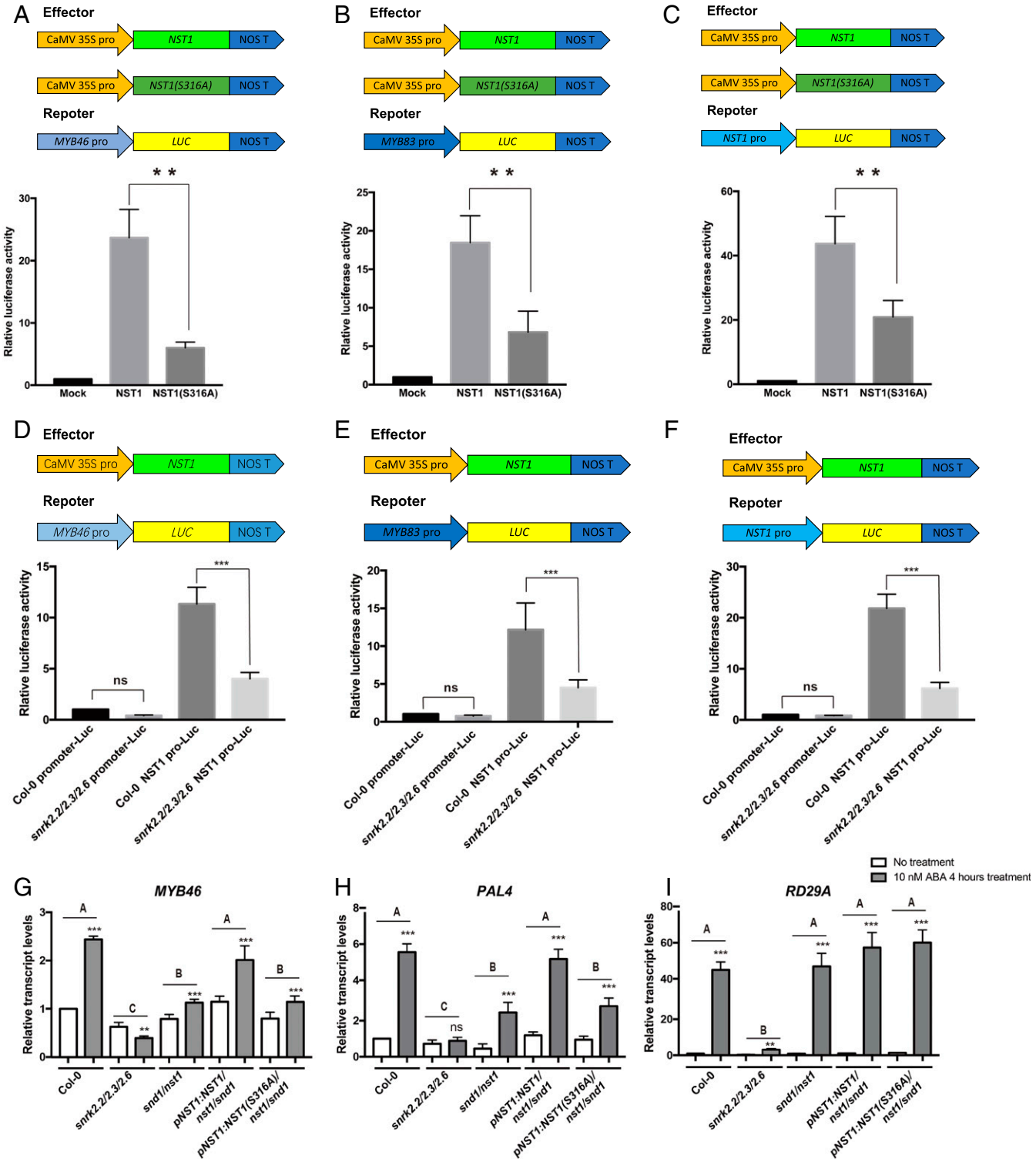

Fig. 6. The phosphorylation site of NST1 is required for its transcriptional activity. (*A*–*C*) Transcriptional activation of (*A*) MYB46, (*B*) MYB83, and (*C*) NST1 promoters by NST1 or NST1$^{(S316A)}$ in wild-type Col-0 protoplasts. (*D*–*F*) Comparison of the transcriptional activation of (*D*) MYB46, (*E*) MYB83, and (*F*) NST1 promoters by NST1 or NST1$^{(S316A)}$ in wild-type Col-0 and *snrk2.2/snrk2.3/snrk2.6* protoplasts. (*G* and *H*) Transcript levels of (*G*) *MYB46*, (*H*) *PAL4*, and (*I*) *RD29A* in 10-wk-old seedlings of wild-type Col-0, *snrk2.2/snrk2.3/snrk2.6* triple mutant, pNST1: NST1 *nst1/snd1* transgenic lines, and pNST1: NST1(S316A) *nst1/snd1* lines with or without 4 h treatment with 10 nM ABA. *ACT2* is employed as the reference gene. Values are reported as relative to wild-type Col-0 and set as 1. Data represent average values ± SD (n = 6 biological replicates). $^{**}P < 0.01$; $^{***}P < 0.0001$ (Student's t test). ns, not significant. In *G* and *H*, the asterisks indicate the significant differences between ABA treatment and no treatment within each accession by Student's t test, and the letters indicate the significant differences of ABA-induced gene expression among different plants ($P < 0.001$) by two-way ANOVA followed by Tukey's multiple comparisons test.

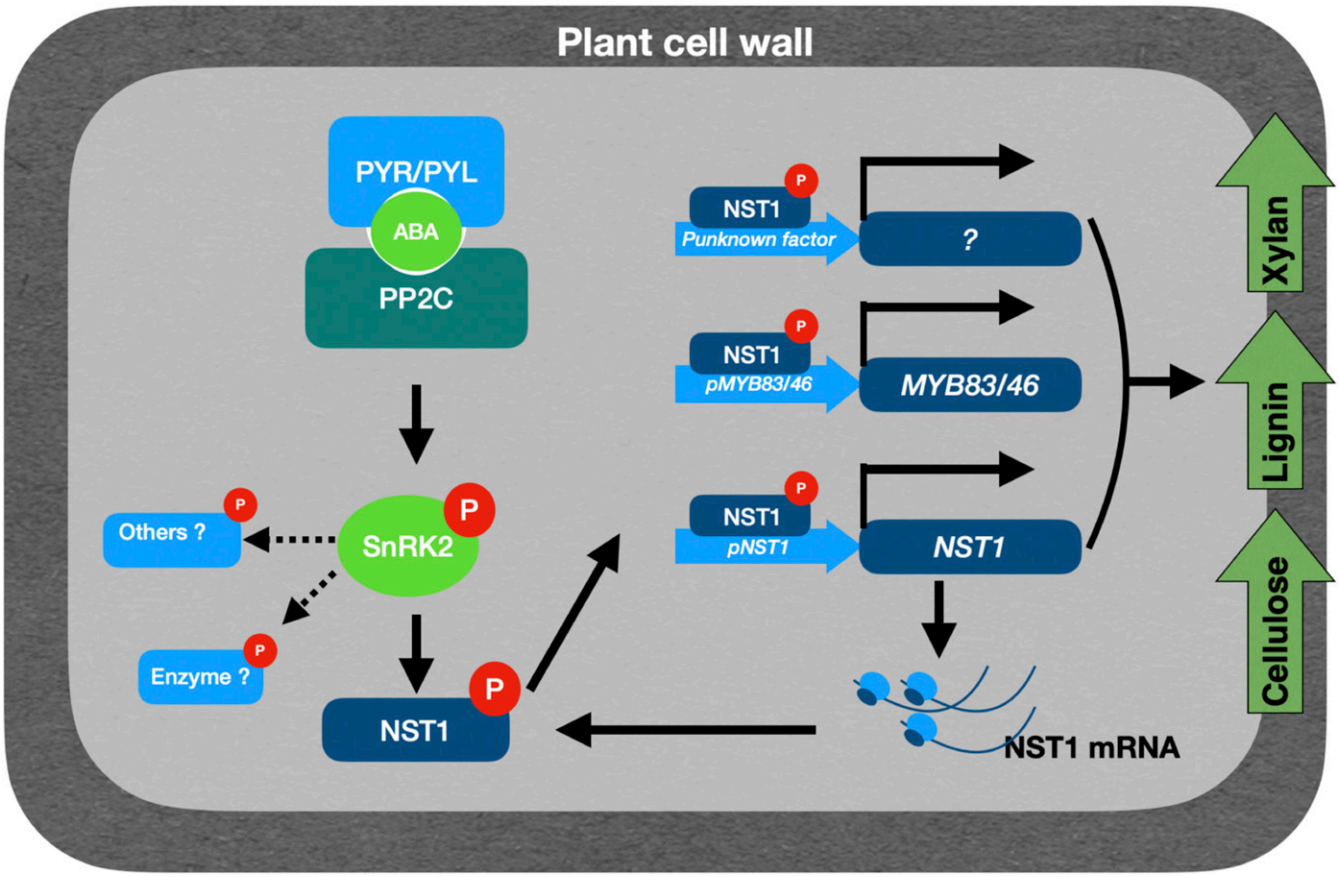

Fig. 7. A model for the role of abscisic acid in the regulation of SCW formation. In the presence of ABA, PP2C binds to PYR/PYL/RCAR proteins and ABA, thereby inhibiting PP2C phosphatase activity. SnRK2s are then activated to phosphorylate the TF NST1, which is a master regulator that binds to promoters to induce the expression of downstream genes, including *MYB83* and *MYB46*. Together with NST1, these TFs can promote lignin, cellulose, and xylan deposition to enhance SCW formation. Future studies should address whether SnRK2s may also activate key enzymes and other proteins involved in SCW formation. P, phosphate.

plants, analysis of ABA levels, cloning of gene constructs, all chemical analytical methods, and details of microscopic assays.

Assay of Protein–Protein Interactions. To identify NST1-interacting proteins, a cDNA library was generated from RNA obtained from 6-wk-old stems of Col-0 wild-type plants. Total RNA was isolated with an RNeasy Plant Mini Kit (Qiagen) and 80 μg RNA were used for messenger RNA (mRNA) purification with a Dynabeads mRNA purification kit (Ambion). The cDNA library was made using both random primers and oligo d(T) with the Make Your Own Mate & Plate Library System (Clontech).

The library was introduced into GAL4 activation domain vector pGADT7-Rec (Clontech). The bait construct was prepared by cloning the coding sequence of NST1 into the GAL4-binding domain vector pGBKT7. The Y187 yeast strain was sequentially transformed with the bait construct and then with the cDNA library following the user manual of the Matchmaker Gold Yeast Two-Hybrid System (Clontech). The transformed yeast were grown on selective medium (*his3*$^-$/*lacZ*$^-$), positive clones were isolated, and the plasmids were sequenced.

Yeast two-hybrid assay was performed as described previously (65) and is further detailed in *SI Appendix*, *Supplementary Materials and Methods*.

For bimolecular fluorescence complementation (BiFC) analysis, the constructs were transformed into *Agrobacterium* strain GV3101, and the resulting strains were used to transform *Nicotiana benthamiana* leaf cells, either individually or in combination (66). The leaves were examined after 48 h of incubation.

To obtain recombinant proteins for in vitro binding assays, the coding sequence of NST1 was cloned into PGEX vector (Amersham) to express the recombinant GST-NST1 fusion protein. The coding sequences of SnRK2.2, SnRK2.3, and SnRK2.6 were constructed in pET28b vector (Novagen), which produced fusion proteins with carboxyl-terminal hexahistidine tags. The primer sequences used for building these constructs are listed in *SI Appendix*, Table S1. *E. coli* BL21 (DE3) cells transformed with the constructs were grown in Luria–Bertani (LB) liquid medium at 37 °C until OD (600) reached 0.7; then 0.1 mM isopropyl β-D-1-thiogalactopyranoside was added to the medium, and the cells were grown at 16 °C for 18 h. After centrifugation, the supernatant was removed, and the bacteria were stored at −80 °C until isolation of the protein.

To investigate the physical interaction between NST1 and SnRK proteins in vitro, Glutathione-Sepharose 4B resin (Thermo Scientific) was incubated with cell lysates of NST1-GST fusion protein or GST protein control for 4 h at 4 °C with constant rotation. The resin was washed three times with 1× phosphate-buffered saline (PBS), and the supernatants were removed. The resins with immobilized GST or NST1-GST proteins were then resuspended in cell lysates of recombinant SnRK2-His_6 proteins for 30 min at room temperature with constant rotation. After five rounds of washing with 1× PBS, the protein complexes were eluted with 2× SDS loading buffer and boiled at 100 °C for 5 min. The eluted proteins were then separated by SDS/PAGE for 1.5 h at 120 V, 150 mA.

In Vitro Phosphorylation Assays. Ni-NTA agarose (Qiagen) and Glutathione-Sepharose 4B resin (Thermo Scientific) were used to purify the recombinant proteins for in vitro binding assays. NST1-GST and $NST1_{(S316A)}$-GST fusion proteins were incubated with or without SnRK2s-6xHis fusion proteins in kinase buffer (50 mM Hepes [pH 7.4], 10 mM $MgCl_2$, 1 mM dithiothreitol, 30 μM ATP) at 30 °C for 2 h. The reaction was stopped and divided into two equal portions. One group of proteins was separated by SDS/PAGE (Thermo-Fisher NuPAGE 4 to 12%, Bis-Tris, 1.5 mm, Mini Protein Gel, 10 well) and stained with Coomassie brilliant blue as the loading control. The other group was also separated by PAGE, and the gel was used for Western blotting with antiphosphoserine antibody (Sigma P5747) to detect phosphorylated proteins.

Dual Luciferase Assays. Protoplasts used in the transient effector-reporter analysis were isolated from 2-wk-old *A. thaliana* seedlings as previously described (61). The coding sequences of NST1 and $NST1_{(S316A)}$ were cloned

into the effector plasmid. The promoters of *MYB83*, *MYB46*, and *NST1* were cloned into the firefly luciferase reporter vector P2GW7 (67). The Renilla luciferase gene driven by the CaMV 35S promoter served as a control to normalize for transformation efficiency. Luciferase activities were measured with a dual-luciferase reporter assay system (Promega).

Bioinformatic Analysis. Alignments generated by the software Geneious R11 with the default parameters MEGA X were used to generate the phylogenetic tree of NST proteins from dicots and monocots. The phylogenetic relationship was inferred with Neighbor-Joining algorithm using 1,000 bootstrap replicates. CLUSTALW2.0 was used to align and analyze the phosphorylation sites among 20 NST1 proteins in dicots. The distribution of amino acid occurrences was visualized using WebLogo (http://weblogo.threeplusone.com/). All the sequences used for analysis were downloaded from National Center for Biotechnology Information and are listed in *SI Appendix*, Table S2.

Data Availability. All study data are included in the article and/or supporting information.

ACKNOWLEDGMENTS. This work was funded by the University of North Texas and the Chinese Academy of Sciences Grant XDB27020104.

1. H. Z. Wang, R. A. Dixon, On-off switches for secondary cell wall biosynthesis. *Mol. Plant* **5**, 297–303 (2012).
2. J. Barros, H. Serk, I. Granlund, E. Pesquet, The cell biology of lignification in higher plants. *Ann. Bot.* **115**, 1053–1074 (2015).
3. M. Kumar, L. Campbell, S. Turner, Secondary cell walls: Biosynthesis and manipulation. *J. Exp. Bot.* **67**, 515–531 (2016).
4. P. E. Marriott, L. D. Gómez, S. J. McQueen-Mason, Unlocking the potential of lignocellulosic biomass through plant science. *New Phytol.* **209**, 1366–1381 (2016).
5. M. Taylor-Teeples *et al*., An Arabidopsis gene regulatory network for secondary cell wall synthesis. *Nature* **517**, 571–575 (2015).
6. R. Zhong, C. Lee, J. Zhou, R. L. McCarthy, Z.-H. Ye, A battery of transcription factors involved in the regulation of secondary cell wall biosynthesis in Arabidopsis. *Plant Cell* **20**, 2763–2782 (2008).
7. J. Zhang, M. Xie, G. A. Tuskan, W. Muchero, J.-G. Chen, Recent advances in the transcriptional regulation of secondary cell wall biosynthesis in the woody plants. *Front. Plant Sci.* **9**, 1535 (2018).
8. C. Plomion, G. Leprovost, A. Stokes, Wood formation in trees. *Plant Physiol.* **127**, 1513–1523 (2001).
9. P. Jenkins, K. Shepherd, Seasonal changes in levels of indole-acetic acid and abscisic acid in stem tissues of *Pinus radiata*. *N. Z. J. Bot.* **4**, 511–519 (1974).
10. T. J. Wodzicki, A. B. Wodzicki, Seasonal abscisic acid accumulation in stem cambial region of *Pinus silvestris*, and its contribution to the hypothesis of a late-wood control system in conifers. *Physiol. Plant.* **48**, 443–447 (1980).
11. M. K. Jensen *et al*., The *Arabidopsis thaliana* NAC transcription factor family: Structure-function relationships and determinants of ANAC019 stress signalling. *Biochem. J.* **426**, 183–196 (2010).
12. S. R. Cutler, P. L. Rodriguez, R. R. Finkelstein, S. R. Abrams, Abscisic acid: Emergence of a core signaling network. *Annu. Rev. Plant Biol.* **61**, 651–679 (2010).
13. A. Sato *et al*., Threonine at position 306 of the KAT1 potassium channel is essential for channel activity and is a target site for ABA-activated SnRK2/OST1/SnRK2.6 protein kinase. *Biochem. J.* **424**, 439–448 (2009).
14. B. Brandt *et al*., Reconstitution of abscisic acid activation of SLAC1 anion channel by CPK6 and OST1 kinases and branched ABI1 PP2C phosphatase action. *Proc. Natl. Acad. Sci. U.S.A.* **109**, 10593–10598 (2012).
15. K. Nakashima *et al*., Three Arabidopsis SnRK2 protein kinases, SRK2D/SnRK2.2, SRK2E/SnRK2.6/OST1 and SRK2I/SnRK2.3, involved in ABA signaling are essential for the control of seed development and dormancy. *Plant Cell Physiol.* **50**, 1345–1363 (2009).
16. H. Fujii, P. E. Verslues, J.-K. Zhu, Identification of two protein kinases required for abscisic acid regulation of seed germination, root growth, and gene expression in Arabidopsis. *Plant Cell* **19**, 485–494 (2007).
17. M. González-Guzmán *et al*., The short-chain alcohol dehydrogenase ABA2 catalyzes the conversion of xanthoxin to abscisic aldehyde. *Plant Cell* **14**, 1833–1846 (2002).
18. H. Fujii, J.-K. Zhu, Arabidopsis mutant deficient in 3 abscisic acid-activated protein kinases reveals critical roles in growth, reproduction, and stress. *Proc. Natl. Acad. Sci. U.S.A.* **106**, 8380–8385 (2009).
19. M. Schmid *et al*., A gene expression map of *Arabidopsis thaliana* development. *Nat. Genet.* **37**, 501–506 (2005).
20. A.-C. Mustilli, S. Merlot, A. Vavasseur, F. Fenzi, J. Giraudat, Arabidopsis OST1 protein kinase mediates the regulation of stomatal aperture by abscisic acid and acts upstream of reactive oxygen species production. *Plant Cell* **14**, 3089–3099 (2002).
21. W.-H. Cheng *et al*., A unique short-chain dehydrogenase/reductase in Arabidopsis glucose signaling and abscisic acid biosynthesis and functions. *Plant Cell* **14**, 2723–2743 (2002).
22. X. Rao, R. A. Dixon, Current models for transcriptional regulation of secondary cell wall biosynthesis in grasses. *Front. Plant Sci.* **9**, 399 (2018).
23. M. Xie *et al*., Regulation of lignin biosynthesis and its role in growth-defense tradeoffs. *Front. Plant Sci.* **9**, 1427 (2018).
24. J. T. Chernys, J. A. Zeevaart, Characterization of the 9-cis-epoxycarotenoid dioxygenase gene family and the regulation of abscisic acid biosynthesis in avocado. *Plant Physiol.* **124**, 343–353 (2000).
25. S. Iuchi *et al*., Regulation of drought tolerance by gene manipulation of 9-cis-epoxycarotenoid dioxygenase, a key enzyme in abscisic acid biosynthesis in Arabidopsis. *Plant J.* **27**, 325–333 (2001).
26. V. Lefebvre *et al*., Functional analysis of Arabidopsis NCED6 and NCED9 genes indicates that ABA synthesized in the endosperm is involved in the induction of seed dormancy. *Plant J.* **45**, 309–319 (2006).
27. P. Wang *et al*., Quantitative phosphoproteomics identifies SnRK2 protein kinase substrates and reveals the effectors of abscisic acid action. *Proc. Natl. Acad. Sci. U.S.A.* **110**, 11205–11210 (2013).
28. N. Mitsuda *et al*., NAC transcription factors, NST1 and NST3, are key regulators of the formation of secondary walls in woody tissues of Arabidopsis. *Plant Cell* **19**, 270–280 (2007).
29. N. Mitsuda, M. Seki, K. Shinozaki, M. Ohme-Takagi, The NAC transcription factors NST1 and NST2 of Arabidopsis regulate secondary wall thickenings and are required for anther dehiscence. *Plant Cell* **17**, 2993–3006 (2005).
30. P. Durek *et al*., PhosPhAt: The *Arabidopsis thaliana* phosphorylation site database. An update. *Nucleic Acids Res.* **38**, D828–D834 (2010).
31. S. D. Yoo, Y. H. Cho, J. Sheen, Arabidopsis mesophyll protoplasts: A versatile cell system for transient gene expression analysis. *Nat. Protoc.* **2**, 1565–1572 (2007).
32. R. Zhong, E. A. Richardson, Z.-H. Ye, Two NAC domain transcription factors, SND1 and NST1, function redundantly in regulation of secondary wall synthesis in fibers of Arabidopsis. *Planta* **225**, 1603–1611 (2007).
33. R. L. McCarthy, R. Zhong, Z.-H. Ye, MYB83 is a direct target of SND1 and acts redundantly with MYB46 in the regulation of secondary cell wall biosynthesis in Arabidopsis. *Plant Cell Physiol.* **50**, 1950–1964 (2009).
34. R. Zhong, E. A. Richardson, Z.-H. Ye, The MYB46 transcription factor is a direct target of SND1 and regulates secondary wall biosynthesis in Arabidopsis. *Plant Cell* **19**, 2776–2792 (2007).
35. Q. Zhang, F. Luo, Y. Zhong, J. He, L. Li, Modulation of NAC transcription factor NST1 activity by XYLEM NAC DOMAIN1 regulates secondary cell wall formation in Arabidopsis. *J. Exp. Bot.* **71**, 1449–1458 (2020).
36. H. Wang, Q. Zhao, F. Chen, M. Wang, R. A. Dixon, NAC domain function and transcriptional control of a secondary cell wall master switch. *Plant J.* **68**, 1104–1114 (2011).
37. Y. Zhao *et al*., Arabidopsis duodecuple mutant of PYL ABA receptors reveals PYL repression of ABA-independent SnRK2 activity. *Cell Rep.* **23**, 3340–3351.e5 (2018).
38. F. Vlad *et al*., Phospho-site mapping, genetic and in planta activation studies reveal key aspects of the different phosphorylation mechanisms involved in activation of SnRK2s. *Plant J.* **63**, 778–790 (2010).
39. M. Boudsocq, M.-J. Droillard, H. Barbier-Brygoo, C. Laurière, Different phosphorylation mechanisms are involved in the activation of sucrose non-fermenting 1 related protein kinases 2 by osmotic stresses and abscisic acid. *Plant Mol. Biol.* **63**, 491–503 (2007).
40. S. Srivastava, R. K. Vishwakarma, Y. A. Arafat, S. K. Gupta, B. M. Khan, Abiotic stress induces change in Cinnamoyl CoA reductase (CCR) protein abundance and lignin deposition in developing seedlings of *Leucaena leucocephala*. *Physiol. Mol. Biol. Plants* **21**, 197–205 (2015).
41. J. Moura-Sobczak, U. Souza, P. Mazzafera, Drought stress and changes in the lignin content and composition in Eucalyptus. *BMC Proc.* **5** (suppl. 7), P103 (2011).
42. M. Yamaguchi *et al*., Regulation of growth response to water stress in the soybean primary root. I. Proteomic analysis reveals region-specific regulation of phenylpropanoid metabolism and control of free iron in the elongation zone. *Plant Cell Environ.* **33**, 223–243 (2010).
43. Y. Hu *et al*., Differential expression of candidate genes for lignin biosynthesis under drought stress in maize leaves. *J. Appl. Genet.* **50**, 213–223 (2009).
44. L. Fan *et al*., Progressive inhibition by water deficit of cell wall extensibility and growth along the elongation zone of maize roots is related to increased lignin metabolism and progressive stelar accumulation of wall phenolics. *Plant Physiol.* **140**, 603–612 (2006).
45. T. Hura, K. Hura, A. Ostrowska, M. Grzesiak, K. Dziurka, The cell wall-bound phenolics as a biochemical indicator of soil drought resistance in winter triticale. *Plant Soil Environ.* **59**, 189–195 (2013).
46. T. Hura *et al*., An increase in the content of cell wall-bound phenolics correlates with the productivity of triticale under soil drought. *J. Plant Physiol.* **169**, 1728–1736 (2012).
47. Z. Lin *et al*., A RAF-SnRK2 kinase cascade mediates early osmotic stress signaling in higher plants. *Nat. Commun.* **11**, 613 (2020).
48. S. Katsuta *et al*., Arabidopsis Raf-like kinases act as positive regulators of subclass III SnRK2 in osmostress signaling. *Plant J.* **103**, 634–644 (2020).
49. Y. Zhou *et al*., Root-specific NF-Y family transcription factor, PdNF-YB21, positively regulates root growth and drought resistance by abscisic acid-mediated indoylacetic acid transport in Populus. *New Phytol.* **227**, 407–426 (2020).
50. J. C. del Pozo, M. B. Boniotti, C. Gutierrez, Arabidopsis E2Fc functions in cell division and is degraded by the ubiquitin-SCF(AtSKP2) pathway in response to light. *Plant Cell* **14**, 3057–3071 (2002).
51. N. G. Taylor, Identification of cellulose synthase AtCesA7 (IRX3) in vivo phosphorylation sites: A potential role in regulating protein degradation. *Plant Mol. Biol.* **64**, 161–171 (2007).

52. C. Sánchez-Rodríguez *et al*., BRASSINOSTEROID INSENSITIVE2 negatively regulates cellulose synthesis in *Arabidopsis* by phosphorylating cellulose synthase 1. *Proc. Natl. Acad. Sci. U.S.A.* **114**, 3533–3538 (2017).
53. J. Gui *et al*., Phosphorylation of LTF1, an MYB transcription factor in Populus, acts as a sensory switch regulating lignin biosynthesis in wood cells. *Mol. Plant* **12**, 1325–1337 (2019).
54. C. Liu, H. Yu, L. Li, SUMO modification of LBD30 by SIZ1 regulates secondary cell wall formation in *Arabidopsis thaliana*. *PLoS Genet.* **15**, e1007928 (2019).
55. J. Mergner *et al*., Mass-spectrometry-based draft of the Arabidopsis proteome. *Nature* **579**, 409–414 (2020).
56. E. G. Allwood, D. R. Davies, C. Gerrish, B. E. Ellis, G. P. Bolwell, Phosphorylation of phenylalanine ammonia-lyase: Evidence for a novel protein kinase and identification of the phosphorylated residue. *FEBS Lett.* **457**, 47–52 (1999).
57. J. P. Wang *et al*., Phosphorylation is an on/off switch for 5-hydroxyconiferaldehyde *O*-methyltransferase activity in poplar monolignol biosynthesis. *Proc. Natl. Acad. Sci. U.S.A.* **112**, 8481–8486 (2015).
58. H. Ooka *et al*., Comprehensive analysis of NAC family genes in *Oryza sativa* and *Arabidopsis thaliana*. *DNA Res.* **10**, 239–247 (2003).
59. S. Puranik, P. P. Sahu, P. S. Srivastava, M. Prasad, NAC proteins: Regulation and role in stress tolerance. *Trends Plant Sci.* **17**, 369–381 (2012).
60. R. Zhong *et al*., Transcriptional activation of secondary wall biosynthesis by rice and maize NAC and MYB transcription factors. *Plant Cell Physiol.* **52**, 1856–1871 (2011).
61. Z. S. Shobbar *et al*., Abscisic acid regulates gene expression in cortical fiber cells and silica cells of rice shoots. *New Phytol.* **178**, 68–79 (2008).
62. L. Xu, W.-H. Shen, Polycomb silencing of KNOX genes confines shoot stem cell niches in Arabidopsis. *Curr. Biol.* **18**, 1966–1971 (2008).
63. Y. Sun *et al*., A ligand-independent origin of abscisic acid perception. *Proc. Natl. Acad. Sci. U.S.A.* **116**, 24892–24899 (2019).
64. K. J. Niklas, *The Evolutionary Biology of Plants* (University of Chicago Press, 1997).
65. J. Gui *et al*., OsREM4. 1 interacts with OsSERK1 to coordinate the interlinking between abscisic acid and brassinosteroid signaling in rice. *Dev. Cell* **38**, 201–213 (2016).
66. K. Schütze, K. Harter, C. Chaban, Bimolecular fluorescence complementation (BiFC) to study protein-protein interactions in living plant cells. *Methods Mol. Biol.* **479**, 189–202 (2009).
67. M. Karimi, D. Inzé, A. Depicker, GATEWAY vectors for Agrobacterium-mediated plant transformation. *Trends Plant Sci.* **7**, 193–195 (2002).